Science Signaling
AAAS

www.sciencesignaling.org/cgi/content/full/1/39/ra6/DC1

Supplementary Materials for

Purinergic Control of T Cell Activation by ATP Released Through Pannexin-1 Hemichannels

Ursula Schenk, Astrid M. Westendorf, Enrico Radaelli, Anna Casati, Micol Ferro, Marta Fumagalli, Claudia Verderio, Jan Buer, Eugenio Scanziani, Fabio Grassi*

*To whom correspondence should be addressed. E-mail: fabio.grassi@irb.unisi.ch

Published 30 September 2008, *Sci. Signal.* **1**, ra6 (2008)
DOI: 10.1126/scisignal.1160583

This PDF file includes:

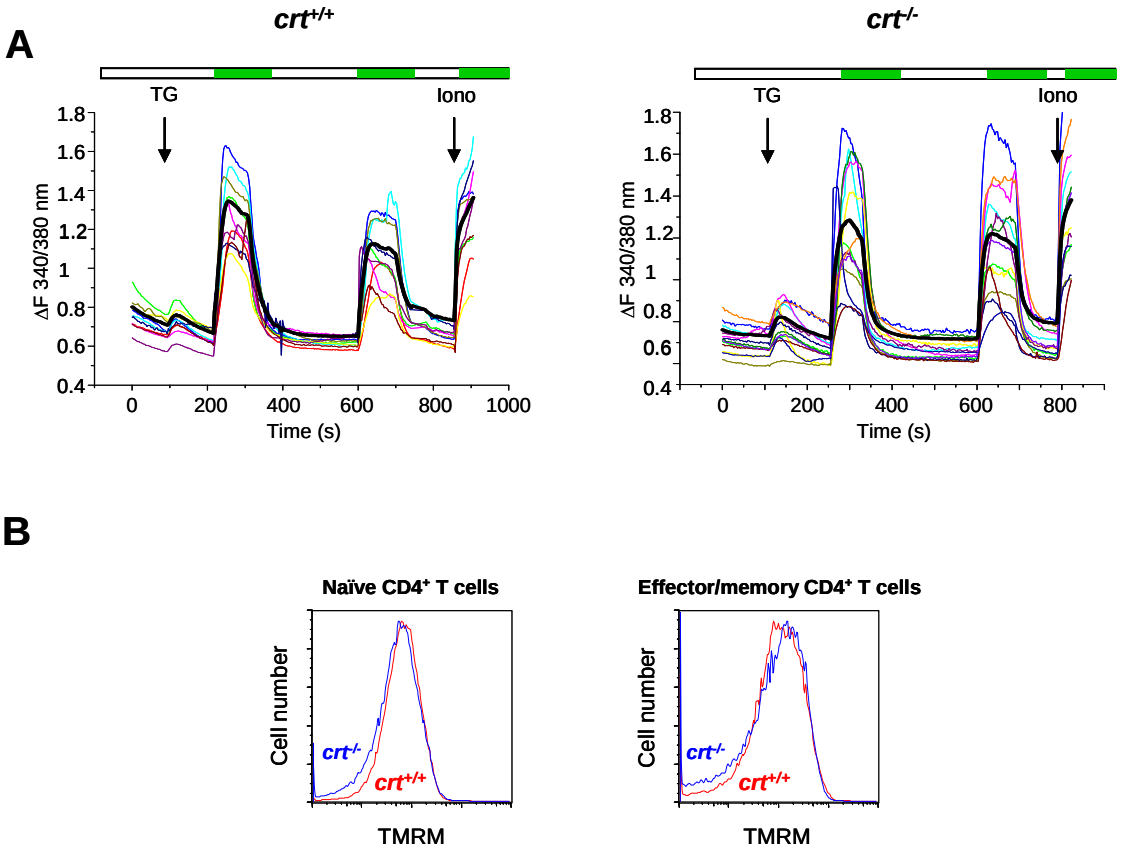

Fig. S1. Decreased CRAC inactivation and unaltered mitochondrial membrane potential in *crt*$^{-/-}$ T cells. (**A**) To score CRAC inactivation, T cells were loaded with Fura-2 and plated on poly-L-lysine–coated coverslips. ER stores of Ca^{2+} were depleted by the addition of thapsigargin (TG) to medium devoid of Ca^{2+}. Following complete ER store depletion, Ca^{2+} was added twice for 100s (green filled bars). Both additions of Ca^{2+} resulted in Ca^{2+} influx through CRACs. Because these channels are inactivated by Ca^{2+}, the second rise in Ca^{2+} occurred with a slower rate and lower amplitude than did the first. *Crt*$^{-/-}$ cells showed diminished CRAC inactivation. Differently colored traces represent Ca^{2+} fluxes in individual cells, whereas the black line represents the average response. Addition of ionomycin at the end of the assay (third green bar) identifies viable cells. (**B**) Tetramethylrhodamine methyl ester (TMRM) staining of sorted naïve ($CD44^{-}CD62L^{+}$) and effector/memory ($CD44^{+}CD62L^{-}$) $CD4^{+}$ T cells from *crt*$^{-/-}$ and *crt*$^{+/+}$ FLC mice showed that deletion of *crt* did not modify mitochondrial membrane potential.

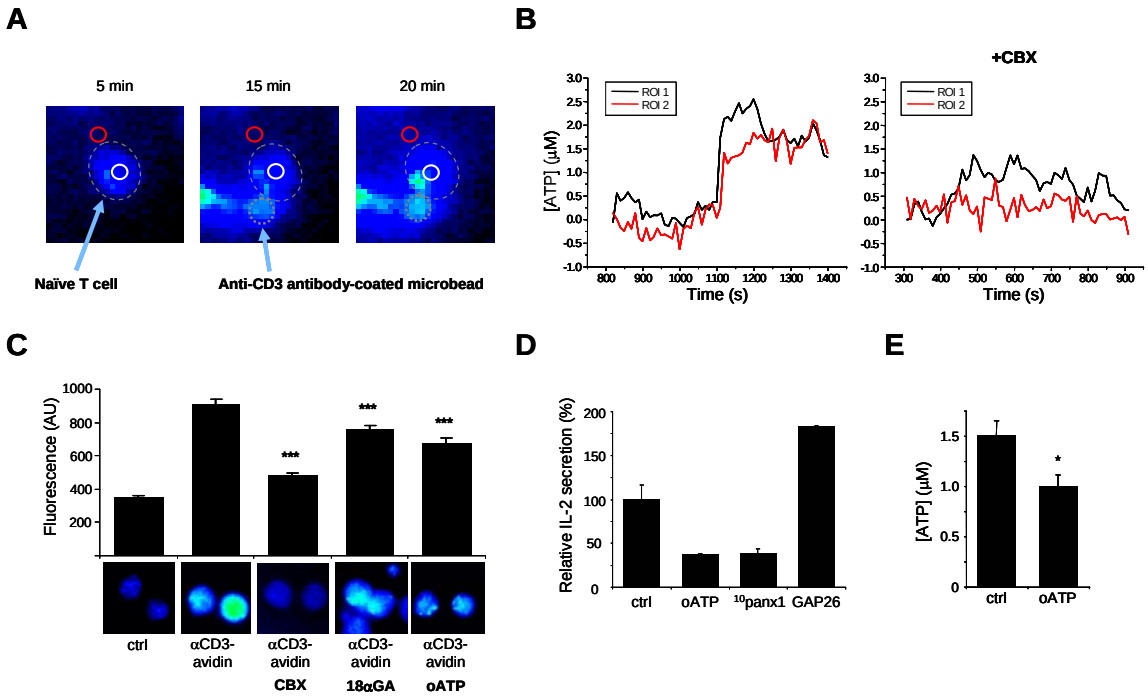

Fig. S2. Analysis of ATP release from activated T cells. (**A**) ATP release from T cells stimulated with anti-CD3 antibody-coated microbeads was measured as the increase in NADPH fluorescence generated by a two-enzyme assay (see Methods). Pseudocolor images show the increased fluorescence in the pericellular region of a naïve $CD4^+$ T cell after synapse formation. (**B**) Representative traces of ATP concentrations in a region of interest (ROI) placed above the T cell (black) or in proximity to the same cell (red). Note that when a T cell is stimulated in the presence of 5 μM carbenoxolone (+CBX, right panel), which inhibits pannexin hemichannels, the fluorescence increase is limited to the cell body (black line), indicative of Ca^{2+}-induced mitochondrial synthesis of NADPH, but no fluorescence is detected in the pericellular region of the same cell (red line). NADPH fluorescence was converted to [ATP] by means of a standard curve, prepared with varying concentrations of ATP as described in the Methods. (**C**) Histograms and pseudocolor images of carboxyfluorescein uptake in $CD4^+$ naïve T cells either untreated or stimulated with cross-linked anti-CD3 antibodies in the absence or presence of the indicated drugs. Three independent experiments were performed (ctrl, n = 141; anti-CD3, n = 142; CBX, n = 224; 18αGA, n = 156; oATP, n = 58). (**D**) Naïve $CD4^+$ T cells were stimulated for 48 h with plate-bound anti-CD3 and anti-CD28 antibodies after which, the amount of IL-2 secreted by these cells into the culture supernatant was determined by ELISA. The pannexin-inhibitory peptide ^{10}panx1, but not the connexin-inhibitory peptide GAP26, inhibited IL-2 secretion comparably to that of oATP. (**E**) Two-enzyme assay of ATP release by naïve $CD4^+$ T cells stimulated with anti-CD3 antibody-coated microbeads. Histograms representing ATP released by cells that were untreated or preincubated with oATP are displayed. *, $P<0.05$; ***, $P<0.0001$.

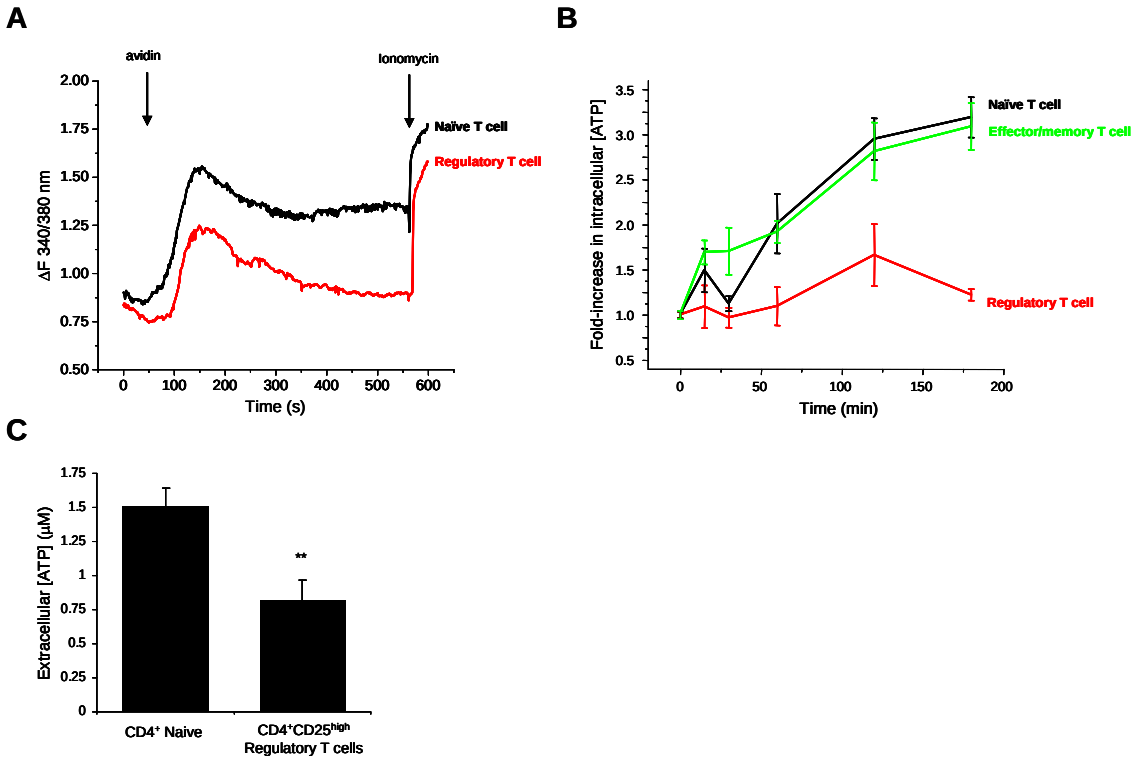

Fig. S3. Reduced Ca^{2+} entry, ATP synthesis, and ATP release in T_{regs}. (**A**) Cytosolic Ca^{2+} profiles after CD3 stimulation of naïve $CD4^+$ T cells and T_{regs}. Note that CCE in T_{reg} cells is more transient and of a lower amplitude than that of naïve $CD4^+$ T cells. (**B**) Changes in the concentrations of cytosolic ATP in sorted naïve and effector/memory $CD4^+$ T cells and T_{regs} at different time points after T cell activation with anti-CD3 antibodies. (**C**) ATP release measured by two-enzyme assay in either naïve $CD4^+$ T cells or T_{regs} stimulated with anti-CD3 antibody-coated beads. **, P <0.01.

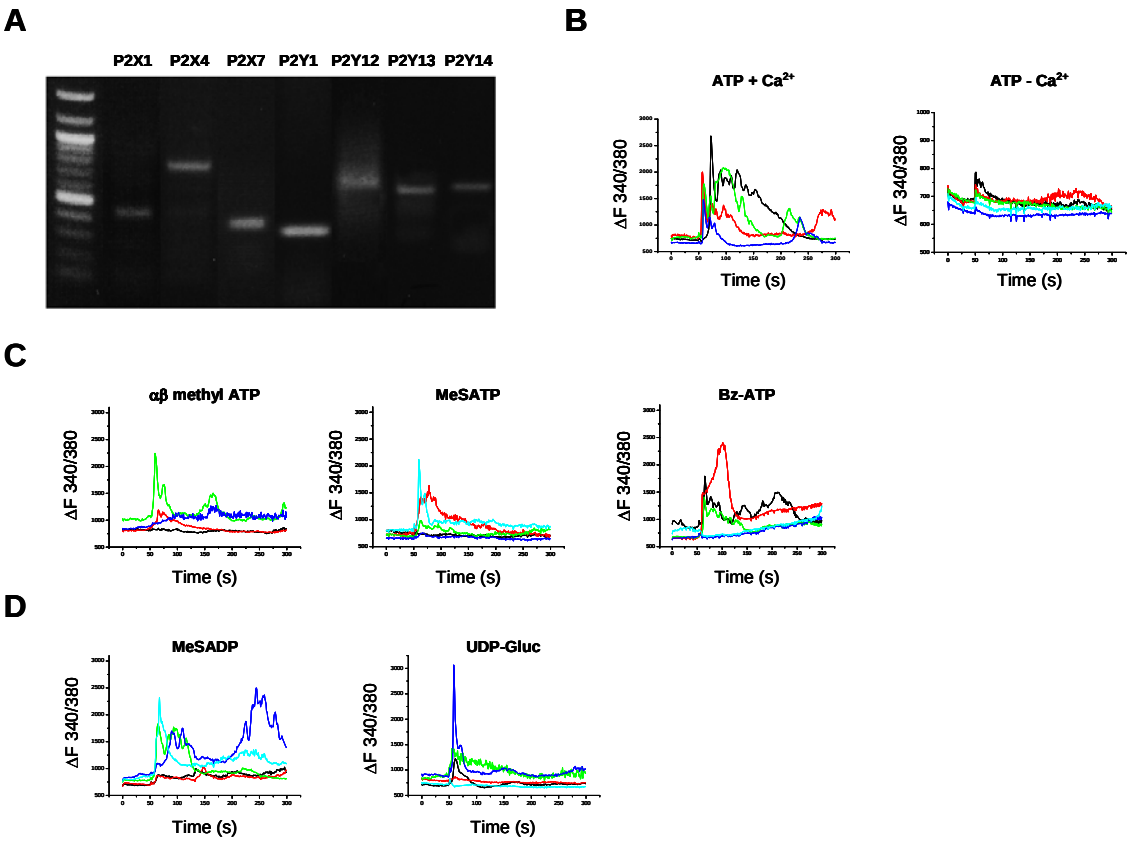

Fig. S4. Analyses of purinergic receptor expression and function in T cells. (**A**) RT-PCR analysis showed that mRNAs for the P2X1, P2X4, and P2X7 receptors and for the P2Y1 and P2Y12 to P2Y14 purinergic receptors are all expressed in T cell clones. (**B**) Ca^{2+} imaging experiments in normal medium (left panel) or medium devoid of Ca^{2+} (right panel) confirm the presence of both ionotropic (P2X) and metabotropic (P2Y) receptors on $CD4^{+}$ T cell clones. (**C**) Preferential agonists for P2X receptors (αβ methyl ATP for P2X1, MeSATP for all P2X receptors, and Bz-ATP for P2X7) confirm the functional competence of the P2X receptors whose expression was detected in A. (**D**) Functional P2Y receptors are also present on T cell clones, as shown by the response to preferential agonists (MeSADP for P2Y1, P2Y12, and P2Y13, UDP-glucose for P2Y14). Differently colored traces represent individual cells monitored in the same field.

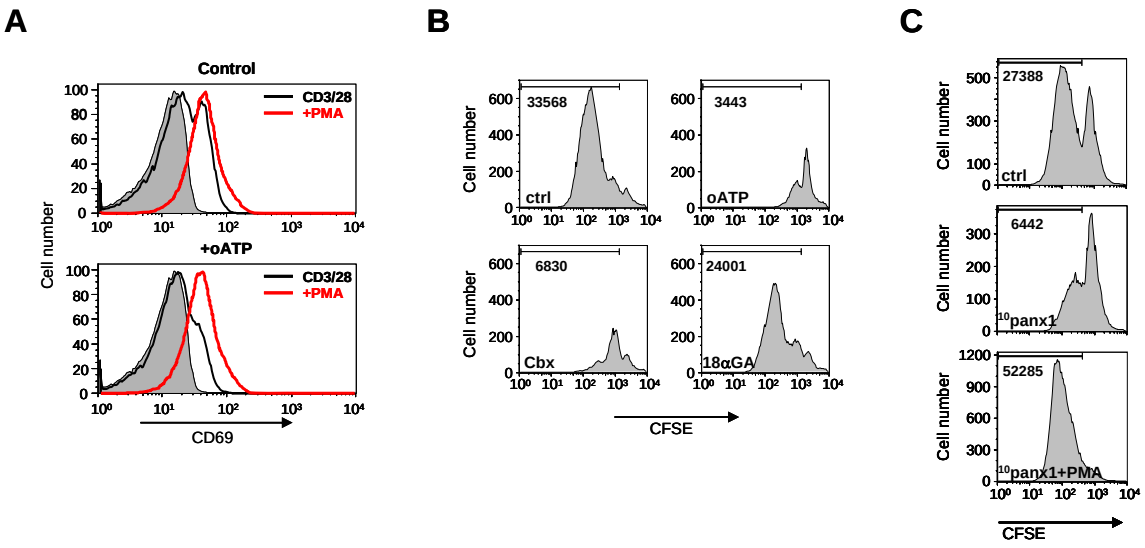

Fig. S5. Influence of oATP and pannexin hemichannel inhibitors on productive T cell activation. (**A**) Antibody labeling of surface CD69 after 6h of stimulation of naïve $CD4^+$ T cells with plate-bound anti-CD3 and anti-CD28 antibodies either in the absence (top panel) or presence (bottom panel) of oATP. The addition of PMA fully restored TCR-stimulated surface CD69 in the presence of oATP. (**B**) T cell proliferation of naïve $CD4^+$ T cells labeled with CFSE and stimulated for 16 h with plate-bound anti-CD3 and anti-CD28 antibodies. Dilution of CFSE (and indicator of cell proliferation) was strongly affected by carbenoxolone (cbx) and oATP, but not by α18-glycyrrhetinic acid. (**C**) ^{10}Panx1 peptide mediated inhibition of T cell proliferation (middle panel) was reversed by the addition of PMA (lower panel).